Fuel-Free Locomotion of Janus Motors: Magnetically Induced Thermophoresis

Larysa Baraban,[†,*] Robert Streubel,[‡,§] Denys Makarov,[‡] Luyang Han,[‡,§] Dmitriy Karnaushenko,[‡] Oliver G. Schmidt,[‡,§] and Gianaurelio Cuniberti[†,⊥]

[†]Max Bergmann Center of Biomaterials, Dresden University of Technology, Budapesterstrasse 27, 01069 Dresden, Germany, [‡]Institute for Integrative Nanosciences, IFW Dresden, Helmholtzstrasse 20, 01069 Dresden, Germany, [§]Material Systems for Nanoelectronics, Chemnitz University of Technology, Reichenhainerstrasse 70, D-09107 Chemnitz, Germany, and [⊥]Division of IT Convergence Engineering, POSTECH, Pohang, Korea

ABSTRACT We present fuel-free locomotion of magnetic spherical Janus motors driven by magnetically induced thermophoresis—a self-diffusive propulsion of an object in any liquid media due to a local temperature gradient. Within this approach an ac magnetic field is applied to induce thermophoretic motion of the objects *via* heating a magnetic cap of the particles, while an additional dc magnetic field is used to orient Janus motors and guide their motion on a long time scale. Full control over the motion is achieved due to specific properties of ultrathin 100-nm-thick Permalloy (Py, $Fe_{19}Ni_{81}$ alloys) magnetic films resulting in a topologically stable magnetic vortex state in the cap structure of Janus motors. Realized here magnetically induced thermophoretic locomotion does not require catalytic chemical reactions that imply toxic reagents. In this respect, we addressed and successfully solved one of the main shortcomings in the field of artificial motors, namely being fully controlled and remain biocompatible. Therefore, our approach is attractive for biotechnological *in vitro* assays and even *in vivo* operations, since the functioning of Janus motors offers low toxicity; it is not dependent on the presence of the fuel molecules in solution. Furthermore, the suggested magnetic ac excitation is superior compared to the previously proposed optically induced heating using lasers as it does not require transparent packaging.

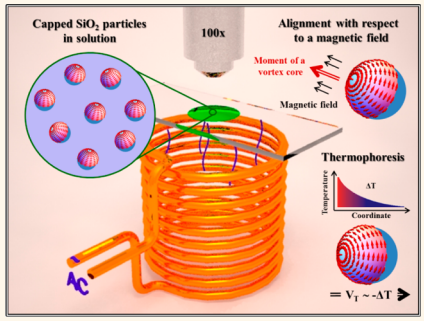

KEYWORDS: fuel-free motors · artificial Janus motors · thermophoresis · hyperthermia

Controlled autonomous motion of micro- and nanoobjects in liquid environments is currently the focus of intense investigations,[1−6] because of its application relevance for biology and medicine,[6−10] for example, for manipulation of cells or pathogenic bacteria circulating in the human body.[11] Targeted drug delivery,[10] hyperthermia[12,13] for cancer treatment, and autonomous microsurgery[14] represent prospective tasks, as well.

Among diverse available concepts enabling the deterministic autonomous motion of the objects at the micro- and nanoscale, catalytic propulsion of the manmade particles was by now one of the most dynamically developing areas in the field of intelligent synthetic nanomachines.[4,5,14−21] Catalytic micro- and nanoengines, capable of deterministic motion, are demonstrated by Janus micro- and nanoparticles,[20,22,23] nanorods,[15,17] or tubular motors[6,8,16,24] that contain ferromagnetic layers for being guided by a magnetic field[18,16,20,21] and a catalytic layer, for example, platinum for maintaining the catalytic chemical reaction in H_2O_2. Although numerous impressive demonstrations of the concept were successfully performed, that is, directed motion[16,17] or transportation of living cells and bacteria,[6,11] the system in its current state has a number of limitations. Catalytically driven artificial motors still suffer from incompatibility of the H_2O_2-based reaction with biological systems, since hydrogen peroxide is a strong oxidizing agent and is harmful to most biological tissues and living cells. Therefore, the mechanism of catalytic motion through tissues still needs to be optimized for the sake of biocompatibility. Hence, there is an intensive seek for alternatives that do not require hydrogen peroxide.

The motion of objects in a liquid environment can be achieved by various phoretic effects, that is, electrophoresis,[25,26] diffusiophoresis,[27−29] or magnetophoresis.[30] An elegant method to achieve autonomous propulsion of the microscopic objects *via* generation of O_2 and H_2 molecules by electric field-assisted redox reactions was recently

* Address correspondence to larysa.baraban@nano.tu-dresden.de.

Received for review October 25, 2012 and accepted December 26, 2012.

Published online December 26, 2012
10.1021/nn305726m

proposed.[26] An approach that can be applied in the biotechnology, that is, for diverse *in vitro* assays,[31] as drug carrier for anticancer therapy[10] or hyperthermia[12] has to offer low toxicity and independence of the synthetic motor on the chemical microenvironment. This task is achieved by exploiting pure physical mechanisms that are not harmful to a human body. For instance, it is well-known that propulsion of the micro- and nanoparticles can be generated by exposing the magnetic object either to a gradient or a rotational magnetic field. It has been shown[5,32−34] that the use of a rotational magnetic field and a magnetic macroscopic object combined with a spiral-type tail results in a self-propulsion of the device in a liquid. Ishiyama *et al*. improved this concept and demonstrated functioning of their devices over a broad range of Reynolds numbers (from 10^{-7} up to 10^{3}) that illustrates the possibility of miniaturization.[35] On the other hand, the potential of thermophoresis of individual colloidal beads was recently reported by several groups that demonstrated self-propelled colloidal particles thermally driven by a defocused laser beam.[36,37] The motion of the particles driven by temperature gradients resembles the Soret effect proportional to the thermal diffusion of the particles and temperature gradient and is reported elsewhere.[37,38] Furthermore the propulsion of nanorods, driven by ultrasound[39] and Al−Ga binary alloy microspheres in water[40] was proposed recently.

Here, we go beyond these established techniques and report on the "fuel-free" generation of directed motion of Janus spheres, which relies on the self-thermophoresis effect combined with the specific magnetic properties of the caps. We achieve directed propulsion without using toxic solutions by localized heating of the metallic cap of the Janus bead, which is realized by applying simultaneously homogeneous applied magnetic field (dc) and alternating (ac) magnetic fields. Figure 1 summarizes the concept of the thermophoreticaly driven Janus particles. An aqueous solution of magnetic Janus spheres is dispensed onto a glass slide, where particles rapidly settle due to gravity. We observe the motion of Janus spheres, located in close proximity to the glass substrate, confined to two dimensions (*xy* plane). The magnetic coil was positioned around the glass substrate that contains the suspension of Janus spheres to generate an alternating magnetic field along *z*-axis (normal to the plane of the glass slide). To generate microscopic temperature gradients that induce locomotion of the Janus beads with a velocity V_T, the frequency and magnitude of the applied ac magnetic field have to be "tuned" to match the specific composition and thickness of the magnetic cap structure to achieve an optimal absorption of the electromagnetic radiation by the metal film. The Janus motors are driven by the temperature difference ΔT formed around the particle due to the local heating of

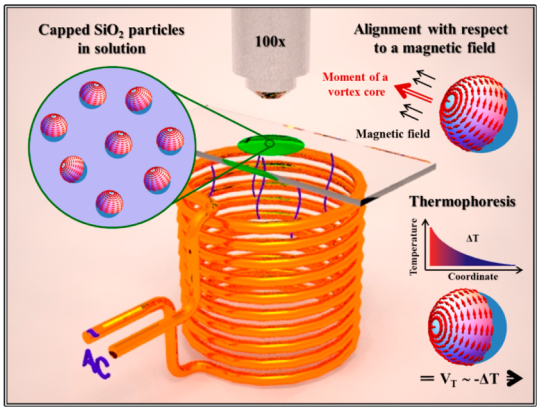

Figure 1. Schematics of the experiment: The motion is visualized by an optical microscope. A coil is positioned around the sample consisting of magnetically capped SiO_2 particles suspended in water. Local distribution of magnetization in the cap structure is schematically shown with arrows. These Janus particles can be aligned with respect to the external magnetic field relying on the interaction between the field and magnetic moment of the vortex core. Propulsion of the particles is due to a thermophoretic force appearing as a result of a temperature difference at both sides of the capped particle exposed to the ac magnetic field of the coil.

the magnetic cap in the applied ac magnetic field. A permanent magnet is used to control the directionality of the motion of self-propelled motors. A similar mechanism by heating magnetic materials was applied earlier for cancer treatment and is known as hyperthermia.[12,13]

Arrays of Janus particles are prepared on SiO_2/Si wafers using a two-step procedure: self-assembly of silica colloidal particles with a diameter of 3 μm on the wafer, followed by deposition of a magnetic layer system.[41] The layer stack consisting of Pt(2 nm)/Py-(100 nm)/Pt(2 nm) is deposited onto the particle templates by magnetron sputtering (details are provided in the Methods section). A scanning electron microscopy (SEM) image of the assembly of capped particles is shown in Figure 2a. The cross-section of a Janus particle is visualized in the inset of Figure 2a after the particle was cut using a focused ion beam (FIB).

The magnetic properties of the samples are derived from longitudinal magneto-optical Kerr effect magnetometry (Figure 2b), which is sensitive to the in-plane magnetization component. The magnetic characterization was carried out at room temperature in an in-plane magnetic field with maxima of ±300 Oe before detaching the particles from the substrate *via* sonication and preparation of aqueous suspension. The magnetic hysteresis loop reveals that the caps are in the so-called magnetic vortex state (inset in Figure 2b),[42] as expected for the chosen thickness of the Py film.[44] The presence of a magnetic vortex in the caps has important implications on the behavior of Janus particles in solution. Vortices are characterized by following two conserved quantities: the polarity, the sense of the vortex core magnetization direction (up or down), and the chirality, the sense of magnetization

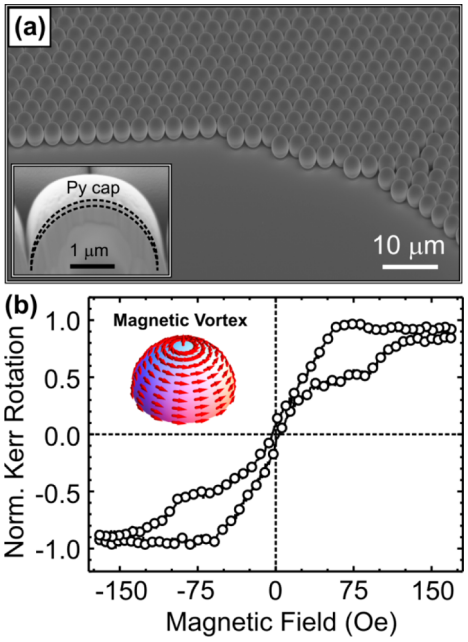

Figure 2. (a) SEM image of the assembly of SiO_2 spherical particles capped with Pt(2 nm)/Py(100 nm)/Pt(2 nm). Diameter of the spheres is 3 μm. Inset in panel a shows the SEM image with the cross-section of a capped sphere cut by FIB. Location of the cap is indicated using dashed lines. (b) Magnetic hysteresis loop measured by means of longitudinal Kerr magnetometry with magnetic field applied parallel to the substrate. The shape of the hysteresis loop is typical for the case when a magnetic vortex is formed in the cap. Magnetic pattern of the vortex is shown in the inset in panel b.

rotation (clockwise or counterclockwise). The curling of the in-plane magnetization leads to a minimized stray field that is crucial to reduce agglomeration of magnetic particles in solution, which is hardly achievable using any other ferromagnetic Janus particles. At the center of the cap an out-of-plane magnetization component appears, which is called vortex core. As follows from the hysteresis loop, the vortex is stable in the field range of $\pm$75 Oe where only a displacement of the vortex core takes place.[43] In a stronger magnetic field of about 170 Oe, the vortex core is expelled from the cap and the vortex is annihilated, resulting in a magnetically saturated state in the Py cap. More details on magnetization reversal in Py caps on spherical particles can be found elsewhere.[44,45]

Owing to the specific magnetization distribution of the vortex, it is magnetically compensated everywhere apart from the location of the vortex core. The presence of this uncompensated component of the vortex allows us to manipulate the orientation of the cap by using a permanent magnet. The strength of the magnetic field at the location of the particles was 40 Oe at maximum, which is sufficiently below the annihilation field of the magnetic vortex (according to hysteresis loop in Figure 2b), meaning that the vortex is linearly displaced from the center of the cap when the field is applied. From our complementary studies of magnetic vortices in cylindrically curved segments with a

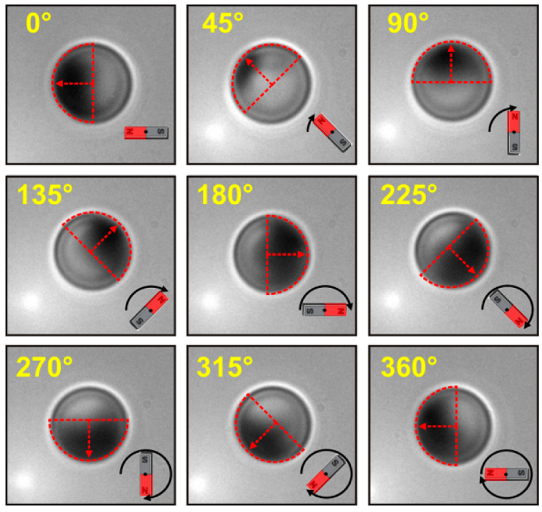

Figure 3. Manipulating the orientation of Janus motors with a diameter of 3 μm by a permanent magnet due to the vortex core magnetization formed within a magnetic cap. Reorientation of the particle is demonstrated in Movie 1 (Supporting Information).

diameter of 1.7 μm, we know that in the field of 40 Oe the displacement of the vortex core is smaller than 0.7 μm.[46] This important finding implies that the vortex core does not change its location on the central region of the particle cap of 3 μm spherical particles upon applying an external dc magnetic field of about 40 Oe, but experiences a torque and will align along the field lines. This provides well-defined anisotropic magnetic properties of the motors and enables us to manipulate the orientation of Janus particles at the microscale using a permanent magnet. Interestingly, the cap will follow the orientation of the magnetic field as shown in Figure 3 (see also Movie 1, Supporting Information). Please note that we did not observe any displacement of the particle during the manipulation experiment, besides the Brownian motion, indicating that the possible gradient of the magnetic field is weak and can be neglected. The manipulations of the Janus spheres and their motion while exposed to an applied dc magnetic field were observed using a video-microscopy setup and recorded with a high-speed camera (Visitron Systems, photometrics cascade 512 B).

It is important to bear in mind that the mechanism behind the change of the orientation of Janus particles with soft magnetic caps is different compared to the recently presented caps consisting of Co/Pt multilayers with perpendicular magnetic anisotropy, where Janus particles are permanently oriented in a dc magnetic field.[20] In the case of Py capped Janus particles, reorientation is achieved by a dynamic process when the magnetic torque is acting on the vortex core (permanent magnet has to be moved with respect to the cap of the particle). In a constant magnetic field the particle will lose its initial orientation along the field lines due to thermal activations. For the Janus particles used in the present work, the time when the particle is

disoriented in an applied dc magnetic field of 40 Oe is about 2 s. Afterward, the particle has to be exposed to the magnetic field again. This seeming disadvantage can be easily overcome when both dc and ac fields are applied. The alternating field is required to achieve thermophoretic motion as discussed below.

Once an ac magnetic field is applied, the magnetic Janus beads are turned into motion with the predefined direction, which is preserved for long times. This motion originates from the heat locally produced within the cap structure, caused by the enhanced absorption of electromagnetic radiation and so-called "hysteretic losses" during ac magnetic field excitation within the Py caps. Thus, a temperature difference ΔT occurs over the surface of the motor, resulting in the propulsive velocity V_T of the Janus motors, which can be defined by a so-called phoretic slip $v_S(\mathbf{r}) \approx -\mathbf{b}\rho(\mathbf{r})\Delta T$ around the particle.[27,29,37] Here, $\rho(\mathbf{r})$ characterizes the density of the fluid along the particle surface; $\mathbf{b}$ is an effective mobility coefficient, which determines the interaction of the fluid particles with the surface of the motors. The velocity V_T can be determined as an integral, over the surface of the particles, of the phoretic slip $v_S(\mathbf{r})$ weighted by complex hydrodynamic resistance matrices.[29]

The thick Py film (100 nm), that was deposited on top of the silica particle array to guarantee the magnetic vortex state, also provides a large amount of spins, which is beneficial in order to achieve a substantial heating of the magnetic part of the Janus particles. In the present experiment, we applied an ac magnetic field in a frequency range between 400 Hz and 6 kHz using a solenoid coil (inner diameter of the coil, 30 mm; diameter of the Cu wire, 0.25 mm; number of windings, 260; dc resistance of the coil, 7.3 Ω; voltage peak-to-peak applied, 10 V). The temperature difference between both sides of the particle, which is the driving force of the thermophoretic motion, can be roughly estimated as follows: First, we calculate the hysteretic losses. From the magnetic hysteresis loop in Figure 2b, we estimate that the total energy required to completely remagnetize the Permalloy cap is about 3 nJ. This energy is calculated as an area under the hysteresis loop taking into account that the saturation magnetization of Permalloy is 870 kA/m. At the frequency of 4 kHz, the energy per second applied to the magnetic cap is 12 μJ/s. This is the upper limit of the power as the used solenoid coil generates the field of about 80 Oe, which is smaller than the saturation field for the Py cap (Figure 2b). Therefore, the actual power supplied to the cap by the ac magnetic field is smaller than the maximum value: $P_0 \approx 6$ μJ/s.

The cap will be heated by the ac excitation if the incoming power P_0 is larger than the dissipated power due to the contact with the surrounding water. The dissipated energy per second, P_d, can be estimated according to the equation: $P_d = \lambda \Delta T_0 S_C / L$, where λ is thermal conductivity of water (0.56 W/(m K)); S_C is the surface area of the cap; L is the distance where the temperature of water decays down to the room temperature; ΔT_0 is the temperature difference of the cap with respect to the room temperature. From the experimental work by Jiang *et al.*,[37] the distance L can be taken as about 5 μm. In this case, ΔT_0 is about 3.7 K. It is important to keep in mind that this value represents the maximal achievable temperature difference, because other factors, like convectional flow, are not accounted for. This simple calculation shows that heating of the cap by an ac magnetic field with a frequency of 4 kHz is possible, but not very efficient. To improve efficiency of heating, higher frequencies of ac field of about 50 kHz are advantageous.

In a similar way, we can estimate the temperature difference between both sides of the cap, ΔT, to be about 1.6 K (in the formula for P_d we used the thermal conductivity of glass (0.8 W/(m K)) and put L equal to the diameter of the SiO_2 particle. Although estimated roughly, the value of ΔT is comparable to the one measured by Jiang *et al.*[37] when Au capped SiO_2 particles were heated by a laser (about 2 K). Now, we can calculate the expected velocity of the Permalloy-capped SiO_2 particle. Assuming a Soret coefficient for Py-SiO_2 of $S_T = 10$ K^{-1} and a diffusion coefficient, D, of about 0.15 $\mu m^2/s$, the velocity of a Janus particle, driven by a temperature difference is equal $V_T = -DS_T\Delta T/3R = 0.34$ μm/s; R is the radius of the particle.[37]

To characterize the observed thermophoretic motion of the Janus motors properly, nonmagnetic plain silica particles of the same size were added to the suspension as references. During experiments we chose the location on the sample to observe a magnetic Janus bead and a reference particle in a single field of view of the microscope. This allows us to compare directly the character of motion of both particles and to extract the thermophoretic motion from drift-related contributions as well as from Brownian random walk. In the following, an analysis of trajectories, velocities, and mean squared displacements (MSDs) of thermally driven Janus motors and a reference particle are presented.

Trajectories of a thermophoretically driven Janus particle and a reference SiO_2 bead, recorded over 40 s, are shown in Figure 4 (see also Movie 2, Supporting Information). The frequency of the applied ac field is set to 4 kHz in this experiment; the strength of the magnetic field is about 80 Oe. Whereas the reference particle fluctuates around its initial position (right-hand side), the Janus sphere reveals a directed motion along the y-axis (left-hand side). This behavior of the magnetic beads in water can be attributed to a positive thermophoresis, as the motion is performed from a hot to a cold region of the particle (away from the magnetic cap). This finding is in agreement with the results reported recently by several groups that investigated the thermophoresis of the Janus particles in water using defocused laser light.[36,37] A similar tendency

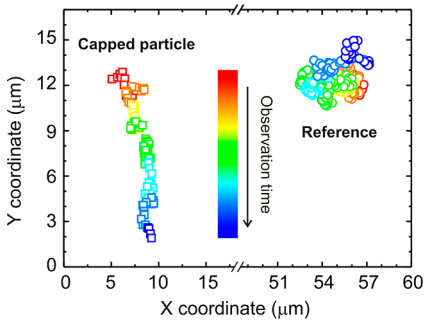

Figure 4. Trajectories of a Janus motor (left) and reference silica particle (right) in an applied ac magnetic field at frequency 4 kHz. Color-coded scale represents the observation time of 40 s.

was observed upon tuning the excitation frequency of the ac field from 400 Hz to 6 kHz (Movies 3, 4 (5 kHz), Supporting Information). As there are no qualitative differences observed in this frequency range, we will focus on the ac excitation with a frequency of 4 kHz.

Obtained trajectories were further evaluated in order to extract information about the velocities of the reference and of the propelled Janus motor. From the trajectory of the Janus sphere (Figure 4), it follows that the directional component of motion experiences strong competition with Brownian fluctuations. To determine the velocity of the magnetic Janus particles, we extract the velocities of both particles *via* plotting the time dependences of the *y* and *x* coordinates (Figure 5a,b). In a similar way, several types of objects (single particles as well as clusters of capped particles) were investigated revealing qualitatively similar behavior to the one discussed in the manuscript. For completeness, tracking of the motion of other Janus particles is presented in the Supporting Information. Generally, velocity of the Janus motors can be also estimated by calculating the instantaneous velocities of the particles from their trajectories. However this method gives precise and reliable results only in the case when the directional component of motion substantially dominates the thermal fluctuations of particle.[16,20] As expected, the reference bead has only a small drift velocity of 0.018 μm/s and 0.01 μm/s along the *y* and *x* direction, respectively. In contrast, driven by the ac magnetic field, the Janus motor is propagating with a velocity of 0.24 μm/s and 0.09 μm/s along the *y* and *x* axes, which is about 1 order of magnitude larger compared to the corresponding velocity components of the reference particle. The experimentally determined velocity of the Janus particle is only slightly smaller compared to the estimation given above. This discrepancy is most probably related to the overestimated temperature difference between both sides of the cap due to neglecting convectional flow around the particle as well as not accounting for Eddy current heating.

It should be noted that this increase in the velocity of the capped particle compared to the reference one is

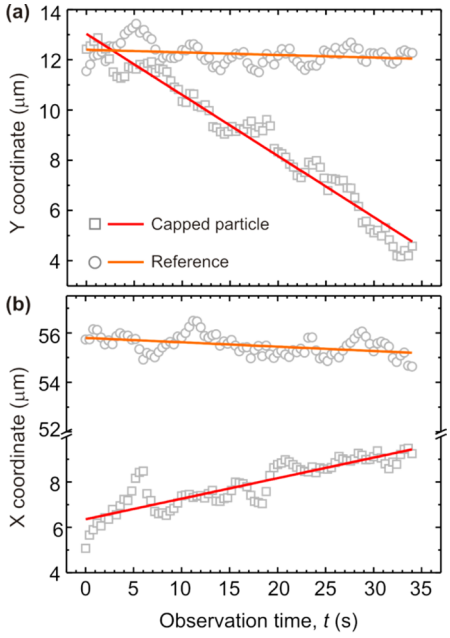

Figure 5. Dependence of (a)*y* and (b)*x* coordinates on time corresponding to the trajectories in Figure 4. Scattered data correspond to the *y* and *x* coordinates of the reference particle, revealing classical Brownian fluctuations, and of the thermophoresis-driven Janus motor in an applied ac magnetic field with an excitation frequency 4 kHz. Solid (orange and red) lines are linear fits to the data. Slope of the lines corresponds to the velocities of the reference particle ($v_{R,x}$ = −0.018 μm/s, $v_{R,y}$ = −0.01 μm/s) and Janus motor ($v_{C,x}$ = 0.091 μm/s, $v_{C,y}$ = −0.243 μm/s).

not due to the gradient magnetic field induced at the edge of the coil. We checked this aspect by observing no displacement of the large agglomerates of Janus spheres in the applied ac magnetic field (Movie 5, Supporting Information), which possess larger net magnetic moment than single particles and therefore should be affected stronger by the gradient magnetic field.

As the 3 μm-sized particles (reference and Janus motor) undergo strong Brownian diffusion, whose scale is comparable to the instantaneous displacement of the Janus motor in an applied magnetic field, it is necessary to calculate the mean squared displacement of both particles to differentiate the self-thermophoresis effect from the drift present in the liquid sample.[47] For this purpose, we performed comparative analysis of the *y* and *x* components of MSDs for the plain silica bead, which is not able to be driven by the ac field, and the Janus motor (Figure 6a,b). Note that we neglect rotational diffusion in the analysis, since the orientation of Janus particles is manipulated by the external permanent magnet. Pure diffusion of the particles on the planar surface is described by MSD = 4*Dt*, where *D* is given by Stokes−Einstein equation.[23] On the basis of the Stokes−Einstein equation, *D* can be calculated to be around 0.16 μm^2/s for particles with a diameter of 3 μm. Deterministic (directed along one of the axes) motion of the Janus motor, propelling with the velocity V_T can then be determined by a simplified analytical

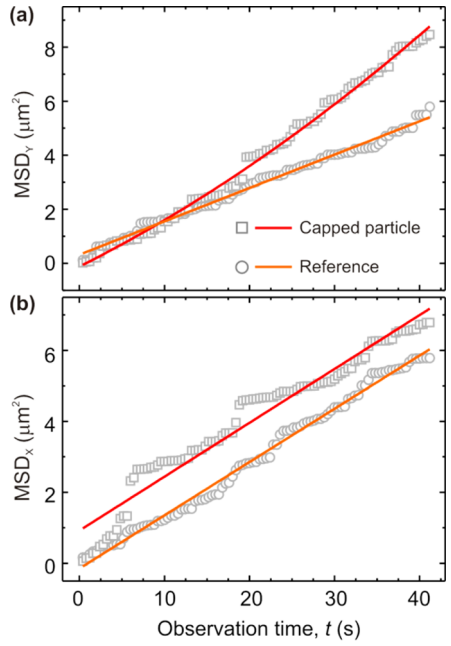

Figure 6. Mean squared displacement of the y (MSD$_Y$) and x (MSD$_X$) coordinates for reference silica particles (circles) and magnetic Janus spheres (squares). (a) MSD$_Y$ reveals parabolic behavior at long time scales for the thermophoretically propelled Janus bead (solid red curve; Fit$_{C,y} = -0.12 + 0.158t + 0.0014t^2$), and stays in linear regime for the reference particle (solid orange curve; Fit$_{R,y} = -0.32 + 0.123t$). Janus motor reveal directed motion in the y-direction. (b) MSD$_X$ of reference and motors spheres with fitting functions Fit$_{C,x} = -0.92 + 0.152t$ (red) and Fit$_{R,x} = -0.15 + 0.151t$ (orange), respectively. Both particles reveal classical Brownian diffusion in the x-direction.

expression for mean squared displacement MSD = $4Dt + V_T^2t^2$, assuming that translational diffusion is substantially more pronounced than the rotational one.

Figure 6a displays the y component of MSD for both analyzed particles. Whereas the MSD$_Y$ of the reference bead follows the Brownian-like diffusion, confirmed by linear fitting (solid orange line), the mean squared displacement of the thermophoretically propelled Janus sphere reveals deterministic motion with parabolic dependence of MSD$_Y$ at long time scale. In contrast, Figure 6b shows linear MSD$_X$ for both particles, the reference one and the Janus bead. This analysis demonstrates that the diffusive behavior of the reference nonmagnetic particle was not affected by the applied ac magnetic field; this results in linear MSD characteristics along x and y axes. On the other hand, the Janus motor exhibits deterministic motion along the y axis, while preserving the Brownian fluctuation along the x coordinate. The experimental data in Figure 6 for the reference particle (MSD$_X$ and MSD$_Y$) as well as the MSD$_X$ for the Janus particle is fitted linearly. Please note that these data were also fit by accounting for a quadratic term. However, its value is of 0.0004(1) μm^2/s^2 at the maximum, which is almost 1 order of magnitude smaller compared to the MSD$_Y$ of the Janus motor.

The estimated velocity of the Janus particle from the MSD$_Y$ is about 0.04 μm/s. It is smaller compared to the one obtained from the analysis of the time dependence of the y-coordinate (0.24 μm/s), which is due to the strong contribution to the motion from the rotational diffusion. The calculated diffusion coefficient D from MSD in our experiment equals 0.05 μm^2/s. It deviates from the value obtained from the Stokes–Einstein approach (0.16 μm^2/s), which might be due to the interaction of the particles with the substrate, for instance, friction forces.

In conclusions, we reported on the realization of a self-thermophoretic motion of magnetic Janus motors in water originating from a local temperature gradient. An ac magnetic field is employed to heat locally the magnetic films deposited on top of the particles. By tuning the parameters of the ac magnetic excitation (amplitude and frequency), the velocity of the carrier particle can be changed. This is crucial to increase the speed of the particles, which is rather low in the present experiments. Furthermore, the selective control over multiple Janus particles can be potentially achieved by varying magnetic properties of the cap structures and adjusting the parameters of the ac magnetic field. In this respect, by varying the saturation magnetization different magnetic hysteresis losses under ac excitation can be achieved, which allows tuning of the heat development in the caps and hence the velocity. Interestingly, these Janus particles can also be used for hyperthermia treatments: once the particles are attached to the tissue guided by the dc field, the amplitude of the ac field is increased in order to produce heat. The accumulation of several particles can ensure sufficient heat generation to overcome a critical temperature for hyperthermia.

This first successful demonstration calls for intensive investigations of the performance of thermophoretically driven Janus particles and their applications in the field of biotechnology. For instance, advanced functionalization of the surface of the Janus motors with specific receptor molecules in combination with optimized high-frequency excitation of the thermophoretic propulsion could help to develop a novel intelligent and biocompatible tool to perform versatile bioanalytical tests, biomolecular sorting, single cells, and genes transportation.

METHODS

Preparation of Pt/Py/Pt Stacks. This step includes magnetron sputter deposition at room temperature of Pt(2 nm)/Py(100 nm)/Pt(2 nm) onto the particle templates. Deposition conditions are as follows: base pressure, 2.0×10^{-7} mbar; Ar sputter pressure, 10^{-3} mbar; deposition rate is about 0.5 Å/s. A composite Fe–Ni alloy target with a composition $Fe_{19}Ni_{81}$ was used for deposition of a Py

layer. Cross-check of the composition after deposition performed using energy dispersive X-ray spectroscopy (EDX) showed composition of the alloy of $Fe_{19}Ni_{81}$ with usual accuracy of the method of ± 1 atom %. Permalloy film is sandwiched by Pt layers to protect the magnetic film from degradation due to oxidation.

Self-Assembled Monolayers of SiO_2 Particles. Preparation of nonmagnetic particle monolayers was carried out following the procedure initially proposed by Micheletto *et al.*[41,48,49] In this case, a droplet of a particle/water solution is deposited onto a cleaned thermally oxidized Si(100) wafer. The cleaning involves ultrasonication in acetone, ethanol, and purified water followed by treatment in oxygen plasma for 4 min. Afterward, the droplet evaporates in a small and tilted box, leading to the self-assembling of the particle monolayers. By varying the concentration of particles in the colloid solution, the tilting angle and the size of the droplet, a sufficient coverage of the substrate with particle monolayers is possible.[50,51]

Conflict of Interest: The authors declare no competing financial interest.

Supporting Information Available: Movie 1 (avi): reorientation of Py Janus particle using applied dc magnetic field. Movie 2 (avi): thermophoresis of the single magnetic Janus particles in an applied ac (4 kHz) and dc magnetic field. Movie 3 (avi): thermophoretic motion of the single magnetic Janus motor in an applied ac (5 kHz) and dc magnetic field. Movie 4 (avi): Thermophoresis of two single particles (ac field at frequency 5kHz). Direction of motion is changed due to the changes of the polarity of the applied dc magnetic field. Movie 5 (avi): displacement of large Janus particle agglomerates in an applied ac magnetic field. Movie 6 (avi): thermophoresis of the single Janus motors, transporting colloidal cargo. Movie 7 (avi): Janus motor transports a colloidal cargo: another particle, attached to the motors surface. Movie 8 (avi): thermophoresis of the cluster of Janus magnetic motors. This material is available free of charge *via* the Internet at http://pubs.acs.org.

Acknowledgment. We greatly acknowledge support from the European Union (European Social Fund) and the Free State of Saxony (Sächsische Aufbaubank) in the young researcher group `InnovaSens' (SAB-Nr. 080942409) and from the German Excellence Initiative *via* the Cluster of Excellence 1056 "Center for Advancing Electronics Dresden" (cfAED). We thank V. Kravchuk (Bogolyubov Institute for Theoretical Physics) for providing the calculation of magnetic state in Permalloy film on spherical particle. Assistance of C. Krien (IFW Dresden) in the deposition of the metal layers is greatly appreciated. This work is financed *via* the German Science Foundation (DFG) Grant MA 5144/1-1 and DFG Research Unit 1713.

REFERENCES AND NOTES

1. Leigh, D. A.; Zerbetto, F.; Kay, E. R. Synthetic Molecular Motors and Mechanical Machines. *Angew. Chem., Int. Ed.* **2007**, *46*, 72–191.
2. Soong, R. K.; Bachand, G. D.; Neves, H. P.; Olkhovets, A. G.; H. G. Craighead, H. G. Montemagno, Powering an Inorganic Nanodevice with a Biomolecular Motor. C. D. *Science* **2000**, *290*, 1555–1558.
3. Leong, T. G.; Randall, C. L.; Benson, B. R.; Bassik, N.; Stern, G. M.; Gracias, D. H. Tetherless Thermobiochemically Actuated Microgrippers. *Proc. Natl. Acad. Sci. U.S.A.* **2009**, *106*, 703–708.
4. Ozin, G. A.; Manners, I.; Fournier-Bidoz, S.; Arsenault, A. Dream Nanomachines. *Adv. Mater.* **2005**, *17*, 3011–3018.
5. Dreyfus, R.; Baudry, J.; Roper, M. L.; Fermigier, M.; Stone, H. A.; Bibette, J. Microscopic Artificial Swimmers. *Nature* **2005**, *437*, 862–865.
6. Sanchez, S.; Solovev, A. A.; Schulze, S.; Schmidt, O. G. Controlled Manipulation of Multiple Cells Using Catalytic Microbots. *Chem. Commun.* **2011**, *47*, 698–700.
7. Tierno, P.; Johansen, T. H.; Fischer, T. M. Transport of Loaded and Unloaded Microcarriers in a Colloidal Magnetic Shift Register. *J. Phys. Chem. B* **2007**, *111*, 13479–13482.
8. Kagan, D.; Campuzano, S.; Balasubramanian, S.; Kuralay, F.; Flechsig, G.-U.; Wang, J. Functionalized Micromachines for Selective and Rapid Isolation of Nucleic Acid Targets from Complex Samples. *Nano Lett.* **2011**, *11*, 2083–2087.
9. Kreuter, J. *Colloidal Drug Delivery Systems*; CRC Press: Boca Raton, FL, 1994.
10. Irwin, D. J. Drug Delivery: One Nanoparticle, One Kill. *Nat. Mater.* **2011**, *10*, 342–343.
11. Campuzano, S.; Orozco, J.; Kagan, D.; Gao, G. M.; Sattayasamitsathit, M.; Claussen, S. J. C.; Merkoçi, A.; Wang, J. Bacterial Isolation by Lectin-Modified Microengines. *Nano Lett.* **2012**, *12*, 396–401.
12. Jordan, A.; Scholz, R.; Maier-Hauff, K.; Johannsen, M.; Wust, P.; Nadobny, J.; Schirra, H.; Schmidt, H.; Deger, S.; Loening, S.; Lanksch, W.; Felix, R. Presentation of a New Magnetic Field Therapy System for the Treatment of Human Solid Tumors with Magnetic Fluid Hyperthermia. *J. Magn. Magn. Mater.* **2001**, *225*, 118–126.
13. Johannsen, M.; Gneveckow, U.; Eckelt, L.; Feussner, A.; Waldöfner, N.; Scholz, R.; Deger, S.; Wust, P.; Loening, S. A.; Jordan, A. Clinical Hyperthermia of Prostate Cancer Using Magnetic Nanoparticles: Presentation of a New Interstitial Tsechnique. *Int. J. of Hyperthermia* **2005**, *21*, 637–647.
14. Solovev, A.; Xi, W.; Gracias, D. H.; Harazim, S.; Deneke, C.; Sanchez, S.; Schmidt, O. G. Self-Propelled Nanotools. *ACS Nano* **2012**, *6*, 1751–1756.
15. Paxton, W. F.; Kistler, K. C.; Olmeda, C. C.; Sen, A.; Angelo, S. K., St.; Cao, Y.; Mallouk, T. E.; Lammert, P. E.; Crespi, V. H. Catalytic Nanomotors: Autonomous Movement of Striped Nanorods. *J. Am. Chem. Soc.* **2004**, *126*, 13424–13431.
16. Solovev, A. A.; Sanchez, S.; Pumera, M.; Mei, Y. F.; Schmidt, O. G. Magnetic Control of Tubular Catalytic Microbots for the Transport, Assembly, and Delivery of Micro-objects. *Adv. Funct. Mater.* **2010**, *20*, 2430–2435.
17. Kline, T. R.; Paxton, W. F.; Mallouk, T. E.; Sen, A. Catalytic Nanomotors: Remote-Controlled Autonomous Movement of Striped Metallic Nanorods. *Angew. Chem., Int. Ed.* **2005**, *44*, 744–746.
18. Pumera, M. Electrochemically Powered Self-Propelled Electrophoretic Nanosubmarines. *Nanoscale* **2010**, *2*, 1643–1649.
19. Dhar, P.; Fischer, T. M.; Wang, Y.; Mallouk, T. E.; Paxton, W. F.; Sen, A. Autonomously Moving Nanorods at a Viscous Interface. *Nano Lett.* **2006**, *6*, 66–72.
20. Baraban, L.; Makarov, D.; Streubel, R.; Moench, I.; Grimm, D.; Sanchez, S.; Schmidt, O. G. Catalytic Janus Motors on Microfluidic Chip: Deterministic Motion for Targeted Cargo Delivery. *ACS Nano* **2012**, *6*, 3383–3389.
21. Burdick, J.; Laocharoensuk, R.; Wheat, P. M.; Posner, J. D.; Wang, J. Synthetic Nanomotors in Microchannel Networks: Directional Microchip Motion and Controlled Manipulation of Cargo. *J. Am. Chem. Soc.* **2008**, *130*, 8164–8165.
22. Valadares, L. F.; Tao, Y. G.; Zacharia, N. S.; Kitaev, V.; Galembeck, F.; Kapral, R.; Ozin, G. A. Catalytic Nanomotors: Self-Propelled Sphere Dimers. *Small* **2010**, *6*, 565–572.
23. Howse, J. R.; Jones, R. A. L.; Ryan, A. J.; Gough, T.; Vafabakhsh, R.; Golestanian, R. Self-Motile Colloidal Particles: From Directed Propulsion to Random Walk. *Phys. Rev. Lett.* **2007**, *99*, 048102.
24. Mei, Y.; Huang, G.; Solovev, A. A.; Bermúdez Ureña, E.; Mönch, I.; Ding, F.; Reindl, T.; Fu, R. K. Y.; Chu, P. K.; Schmidt, O. G. Versatile Approach for Integrative and Functionalized Tubes by Strain Engineering of Nanomembranes on Polymers. *Adv. Mater.* **2008**, *20*, 4085–4090.
25. Ryzhkova, A. V.; Podgornov, F. V.; Haase, W. Nonlinear Electrophoretic Motion of Dielectric Microparticles in Nematic Liquid Crystals. *Appl. Phys. Lett.* **2010**, *96*, 151901.
26. Loget, G.; Kuhn, A. Electric Field-Induced Chemical Locomotion of Conducting Objects. *Nat. Commun.* **2011**, *2*, 535.
27. Baraban, L.; Tasinkevych, M.; Popescu, M. N.; Sanchez, S.; Dietrich, S.; Schmidt, O. G. Transport of Cargo by Catalytic Janus Micro-Motors. *Soft Matter* **2012**, *8*, 48–52.
28. Ebbens, S. J.; Howse, J. R. In Pursuit of Propulsion at the Nanoscale. *Soft Matter* **2010**, *6*, 726–738.

29. Popescu, M. N.; Dietrich, S.; Tasinkevych, M.; Ralston, J. Phoretic Motion of Spheroidal Particles Due to Self-Generated Solute Gradients. *Eur. Phys. J. E* **2010**, *31*, 351–367.
30. Lim, J.-K.; Lanni, C.; Evarts, E. R.; Lanni, F.; Tilton, R. D.; Majetich, S. A. Magnetophoresis of Nanoparticles. *ACS Nano* **2011**, *5*, 217–226.
31. Baudry, J.; Rouzeau, C.; Goubault, C.; Robic, C.; Cohen-Tannoudji, L.; Koenig, A.; Bertrand, E.; Bibette, J. Acceleration of the Recognition Rate between Grafted Ligands and Receptors with Magnetic Force. *Proc. Natl. Acad. Sci. U.S.A.* **2006**, *103*, 16076–16078.
32. Honda, T.; Arai, K. I.; Ishiyama, K. Micro Swimming Mechanisms Propelled by External Magnetic Fields. *IEEE Trans. Magn.* **1996**, *32*, 5085–5087.
33. Fischer, P.; Ghosh, A. Magnetically Actuated Propulsion at Low Reynolds Numbers: Towards Nanoscale Control. *Nanoscale* **2011**, *3*, 557–563.
34. Smith, E. J.; Makarov, D.; Sanchez, S.; Fomin, V. M.; Schmidt, O. G. Magnetic Microhelix Coil Structures. *Phys. Rev. Lett.* **2011**, *107*, 097204.
35. Gutfleisch, O.; Bollero, A.; Handstein, A.; Hinz, D.; Kirchner, A.; Yan, A.; Mueller, K.-H.; Schultz., L. Nanocrystalline High Performance Permanent Magnets. *J. Magn. Magn. Mater.* **2002**, *242*, 1277–1283.
36. Volpe, G.; Buttinoni, I.; Vogt, D.; Kümmerer, H. G.; Bechinger, C. Microswimmers in Patterned Environments. *Soft Matter* **2011**, *7*, 8810–8815.
37. Jiang, H.-R.; Yoshinaga, N.; Sano, M. Active Motion of Janus Particle by Self-Thermophoresis in Defocused Laser Beam. *Phys. Rev. Lett.* **2010**, *105*, 268302.
38. Weinert, F. M.; Braun, D. Observation of Slip Flow in Thermophoresis. *Phys. Rev. Lett.* **2008**, *101*, 168301.
39. Wang, W.; Castro., L. A.; Hoyos, M.; Mallouk, T. E. Autonomous Motion of Metallic Microrods Propelled by Ultrasound. *ACS Nano* **2012**, *6*, 6122–6132.
40. Gao, W.; Pei, A.; Wang, J. Water-Driven Micromotors. *ACS Nano* **2012**, *6*, 8432–8438.
41. Micheletto, R.; Fukuda, H.; Ohtsu, M. A. A Simple Method for the Production of a Two-Dimensional, Ordered Array of Small Latex Particles. *Langmuir* **1995**, *11*, 3333–3336.
42. Choe, S. B.; Acremann, Y.; Scholl, A.; Bauer, A.; Doran, A.; Stöhr, J.; Padmore, H. A. Vortex Core-Driven Magnetization Dynamics. *Science* **2004**, *304*, 420–422.
43. Streubel, R.; Kravchuk, V. P.; Sheka, D. D.; Makarov, D.; Kronast, F.; Schmidt, O. G.; Gaididei, Y. Equilibrium magnetic states in individual hemispherical permalloy caps. *Appl. Phys. Lett.* **2012**, *101*, 132419.
44. Streubel, R.; Makarov, D.; Kronast, F.; Kravchuk, V.; Albrecht, M.; Schmidt, O. G. Magnetic Vortices on Closely Packed Spherically Curved Surfaces. *Phys. Rev. B* **2012**, *85*, 174429.
45. Kravchuk, V. P.; Sheka, D. D.; Streubel, R.; Makarov, D.; Schmidt, O. G.; Gaididei, Y. Out-of-Surface Vortices in Spherical Shells. *Phys. Rev. B* **2012**, *85*, 144433.
46. Streubel, R.; Thurmer, D. J.; Makarov, D.; Kronast, F.; Kosub, T.; Kravchuk, V.; Sheka, D. D.; Gaididei, Y.; Schäfer, R.; Schmidt, O. G. Magnetically Capped Rolled-up Nanomembranes. *Nano Lett.* **2012**, *12*, 3961–3966.
47. Dunderdale, G.; Ebbens, S.; Fairclough, P.; Howse, J. Importance of Particle Tracking and Calculating the Mean-Squared Displacement in Distinguishing Nanopropulsion from Other Processes. *Langmuir* **2012**, *28*, 10997–11006.
48. Baraban, L.; Makarov, D.; Albrecht, M.; Rivier, N.; Leiderer, P.; Erbe, A. Frustration-Induced Magic Number Clusters of Colloidal Magnetic Particles. *Phys. Rev. E* **2008**, *77*, 031407.
49. Baraban, L.; Erbe, A.; Leiderer, P. Characterisation of Magnetic Colloids by Means of Magnetooptics. *Eur. Phys. J. E* **2007**, *23*, 129–133.
50. Brombacher, C.; Saitner, M.; Pfahler, C.; Plettl, A.; Ziemann, P.; Makarov, D.; Assmann, D.; Siekman, M.; Abelmann, L.; Albrecht, M. Tailoring Particle Arrays by Isotropic Plasma Etching: An Approach Towards Percolated Perpendicular Media. *Nanotechnology* **2009**, *20*, 105304–195309.
51. Makarov, D.; Bermúdez-Ureña, E.; Schmidt, O. G.; Liscio, F.; Maret, M.; Brombacher, C.; Schulze, S.; Hietschold, M.; Albrecht, M. Nanopatterned CoPt Alloys with Perpendicular Magnetic Anisotropy. *Appl. Phys. Lett.* **2008**, *93*, 153112.